Theor. Appl. Climatol. 54, 39–46 (1996)

Theoretical and Applied Climatology

USDA-ARS, Wind Erosion Research Unit, Kansas State University, Manhattan, Kansas, U.S.A.

Crop Residue Effects on Aerodynamic Processes and Wind Erosion*

L. J. Hagen

With 6 Figures

Received August 5, 1994
Revised March 20, 1995

Summary

This study focuses on both the mechanisms and degree of wind erosion control that various residue levels provide. First, scale parameters of Weibull wind-speed distributions at meteorological stations were modified to predict friction velocity distributions at eroding field sites. Simplified erosion prediction equations then were used to evaluate wind erosion on highly erodible, loose, sandy soils. Parameters for the erosion prediction equations were developed from wind tunnel data on soil loss and threshold friction velocities at various residue levels. Erosion-control mechanisms of flat residue include restricting soil emission from the surface and increasing threshold wind speeds. A minimum of 30 to 60 percent flat cover is needed to provide adequate control on highly erodible sands. The control level by flat residue can be increased by using short fields. Erosion-control mechanisms of standing residue include reducing the soil-surface friction velocity and intercepting saltating soil. Standing residue is more effective than flat residue, and 5 percent vertical silhouette area of standing residue per unit horizontal area provides adequate erosion-control in low and moderate wind regimes.

1. Introduction

Crop residue affects the heat, mass, and momentum exchange between the earth's surface and the atmosphere. The focus in this paper will be on quantifying the reduction of momentum transfer to the soil by the intervening crop residue and the subsequent calculation of wind erosion.

Currently, the effect of residue on wind erosion generally is assessed using the empirical relations in the Wind Erosion Equation (WEQ) (Woodruff and Siddoway, 1965). The WEQ uses type, orientation, and air-dry mass of residue as inputs. However, new technology is being developed to predict wind erosion on a physical basis (Hagen, 1991a), describing residue on the surface in terms of fraction of soil cover. Standing residues are described in terms of vertical distribution of leaf area and stalk/stem silhouette area per unit horizontal soil surface area. These residue variables were selected, because they are related physically to level of wind erosion protection. Useful relationships to convert standing stalk area to random surface cover were developed by Gregory (1982).

The major data on residue effects on wind erosion come from wind tunnel studies. Among these data are soil loss measurements from a tray protected with various levels of simulated or real residue in a flat or standing orientation (Fryrear, 1985; Lyles and Allison, 1981; van de Ven, Fryrear, and Spaan, 1989). The tray data often area presented as a ratio of protected-to-bare tray soil loss (SLR). Unfortunately, the SLR varies with the treatment wind speed (Siddoway, Chepil, and Armbrust, 1965). Little research has focused

* Contribution from USDA, ARS in cooperation with Kansas Agricultural Experiment Station, Contribution Number 95-41-J.

on how SLR results should be interpreted to predict wind erosion on agricultural fields.

Wind tunnel data also include measurements of the threshold friction velocities at which soil movement begins under various levels of surface protection (Marshall, 1971; Lyles and Allison, 1976; Raupach et al., 1993). Again, little research has considered the use of these data to predict wind erosion.

In order to interpret the wind tunnel data and ultimately determine the reduction in field wind erosion over time by various residue levels, one can follow a sequence of systematic steps. First, a climatic data base with the relevant wind information must be obtained from a meteorological station. Second, aerodynamic roughness of both the station and the field must be calculated from physical parameters that describe their respective underlying surfaces. Third, the magnitude of the wind distribution from meteorological stations must be modified, when a significant difference exists in surface aerodynamic roughness between the station and the field where erosion is to be assessed. Fourth, wind erosion rates must be determined from the total momentum transfer to the field surface by partitioning it between the soil and residue. Finally, wind erosion must be integrated over the wind regime of interest.

The objective of this study was to illustrate wind erosion reduction caused by flat and standing residue on a simple field for a range of wind regimes.

2. Theory and Methods

2.1 Wind Data Base

The transport capacity of loose, saltating soil by wind is proportional to the wind power (i.e., wind speed cubed) for speeds above the saltation threshold (Greeley and Iverson, 1985). Because the transport capacity is highly sensitive to wind speed, a high quality wind data base is essential for assessing impact of residue on wind erosion.

For the United States, researchers at Battelle Northwest Laboratory prepared a Wind Energy Resource Information System (WERIS) data base summarizing 900 locations (Elliot et al., 1987). The WERIS data base contains tables of joint wind speed/direction frequency by month. Using these tables, Skidmore and Tatarko (1991) adjusted all wind speeds to a 10-m reference height, according to the following (Elliot, 1979)

$$u_2 = u_1 \left(\frac{z_2}{z_1}\right)^{1/7} \tag{1}$$

where u_1 and u_2 = wind speeds at height z_1 and z_2, respectively.

Next, they eliminated the calm periods and calculated scale and shape parameters for the Weibull distribution function (Apt, 1976) for each of the 16 cardinal wind directions by month. The Weibull probability density function of wind speeds, $f(u)$, is defined by

$$f(u) = \left(\frac{k}{c_W}\right)\left(\frac{u}{c_W}\right)^{k-1} \exp\left[-\left(\frac{u}{c_W}\right)^{k}\right] \tag{2}$$

where u = wind speed (L/T), c_w = scale parameter (L/T), and k = shape parameter (dimensionless).

Locations with less than 5 years of wind data were eliminated from the analyses.

Weibull wind parameters over all directions at two sites in different wind regimes were selected for examples in this study, because each site has nearby, highly erodible, sandy soils. The sites were Lubbock, Texas in March ($c_w = 7.62$ m/s, $k = 2.60$) and Wausau, Wisconsin in May ($c_w = 5.52$, $k = 2.49$).

2.2 Aerodynamic Roughness and Momentum Transfer

In the atmosphere, an inertial sublayer (logarithmic layer) occupies the zone from about twice the residue height upward to 15 percent of the boundary layer depth. In the inertial sublayer, the wind speed profile is described by (Panofsky and Dutton, 1984)

$$u(z) = \left(\frac{u_*}{k}\right) \ln \frac{z-d}{z_0} + \psi \tag{3}$$

where $u(z)$ = wind speed at height z above soil surface (L/T), u_* = friction velocity (L/T), k = von Karman's constant (0.4), z_0 = aerodynamic roughness length (L), d = displacement height (L), ψ = thermal stability term (L/T)

Under near neutral stability, which is typical with the high wind speeds during wind erosion events, ψ is near zero. The friction velocity is related to the downward momentum transfer (τ) as

$$\tau = \rho u_*^2 \tag{4}$$

where

$$\rho = \text{air density}\left(\frac{M}{L^3}\right) \tag{5}$$

The friction velocity at the field drives the erosion process. Hence, it is necessary to determine the friction velocity distribution at the field. The shape parameter of the Weibull wind-speed distribution calculated for the station will remain unchanged at the field, but the scale parameter often must be modified. By applying Eq. (3), the wind speed log-law, the scale parameter for friction velocity, c_{*w}, at the station is

$$c_{*w} = \frac{0.4 c_W}{\ln\left[\dfrac{z-d}{z_{0W}}\right]} \tag{6}$$

where the subscript w denotes weather station parameters.

When the roughness at the station and the field are significantly different, the station scale parameter must be corrected. Panofsky and Dutton (1984) reviewed the necessity for such a correction and also provided equation to calculate it. For high winds and neutral stability, a numerical approximation of their equations gives

$$c_* = c_{*W}\left(\frac{z_0}{z_{oW}}\right)^{0.067} \tag{7}$$

A typical roughness length is $z_{ow} = 25\,\text{mm}$ at airport areas where meteorological stations often are located (Panofsky and Dutton, 1984). This value was used as the station roughness length in calculating the results.

The z_0 of the field surface can vary considerably, but erodible fields are generally smoother than the station surface. In a wind tunnel test, wheat stubble with 3.5 mm mean diameter (D) was placed on a smooth sand surface in a flat, random orientation over the 16 m length of the working section. The wind tunnel has a 1.52×1.82 m cross-section and has been described previously (Lyles and Allison, 1981). Measured values of z_0/D increased from 0.08 to 0.16 as residue cover increased from 6 to 31 percent. These values represent the minimum roughness lengths that might be encountered with flat residue cover. Erosion increased the roughness of the surface. A z_0 of 5 mm was selected for flat cover and bare soil to calculate field results.

The z_0 for standing residue generally scales with residue height, h, and increases slightly with residue diameter (Shaw and Pereira, 1982). The increase with diameter is caused by a corresponding increase in scale of eddies generated in the stalk wake. For stalks without leaves, the silhouette area per unit horizontal surface area (SAI) is

$$\text{SAI} = nDh \tag{8}$$

where n = number of stalks per unit area ($1/L^2$), D = stalk diameter (L), and h = stalk height (L).

A prediction equation that relates z_0/h to SAI and D is (Hagen and Armbrust, 1994)

$$\frac{zo}{h} = \frac{1}{A + \dfrac{B\ln(\text{SAI})}{\text{SAI}} + \dfrac{C}{\text{SAI}}} \tag{9}$$

where $A = 28.41 - 3.72\ln(D)$, $B = -3.052 + 0.6\ln(D)$, $C = -8.33 + 1.54\ln(D)$

Obviously, the minimum value of z_0 from Eq. (9) is restricted to that of the underlying soil surface. An example of results from Eq. (9) was plotted and compared to data collected in other wind tunnels, as reported by Raupach (1992) (Fig. 1). The prediction equation and data are in reasonable agreement, particularly at SAI less than 0.1, which is of most interest in wind erosion.

2.3 *Wind Erosion Prediction*

On agricultural soils, the general wind erosion process can be modeled as the time-dependent conservation of mass with two sources of erodible material (emission and abrasion) and two sinks (trapping and suspension), Hagen (1991b). To reduce the complexity for this discussion, we will consider only a uniform field with a surface consisting mainly of loose-erodible sand. For such a system in quasi-steady state with one-dimensional flow, the conservation equations reduce to the form:

$$\frac{dq}{dx} = c_{en}(q_c - q) \tag{10}$$

where q = saltation discharge (M/LT), x = distance from upwind nonerodible boundary along wind direction (L), q_c = saltation discharge transport capacity (M/LT), and c_{en} = emission coefficient of bare sand (1/L).

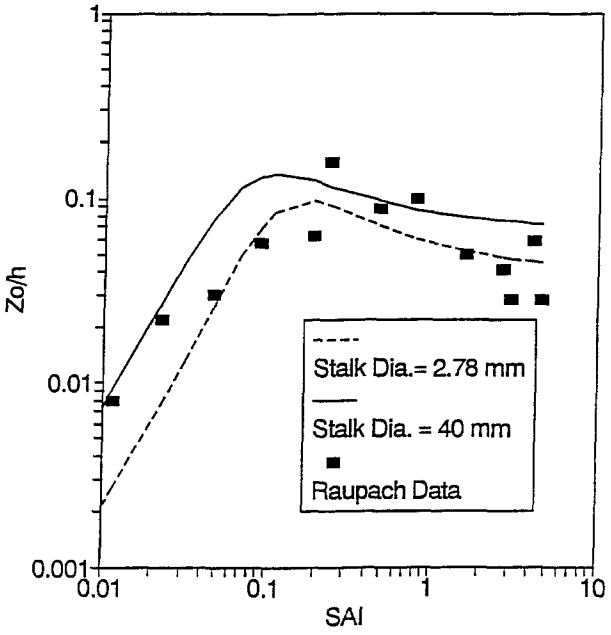

Fig. 1. Predicted (Eq. 9) and measured (Raupach, 1992) aerodynamic roughness as a function of standing residue silhouette area

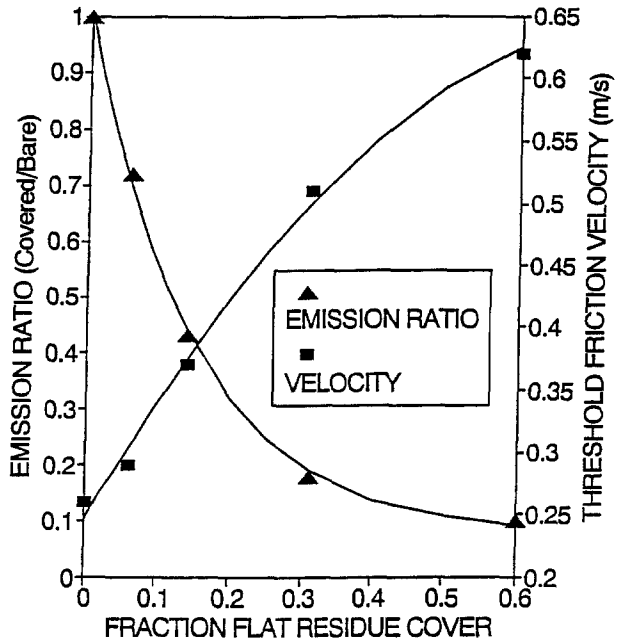

Fig. 2. Measured ratio of emission coefficients for covered and bare soils and dynamic threshold friction velocities as a function of flat residue cover

Although Eq. (10) is simplified greatly from the general erosion equations, it does represent an important segment of erosion problems in which crops are grown on sandy soils with little aggregate structure. Moreover, maintaining residue is frequently the only viable wind erosion control on such soils. Field measurements also demonstrate that on a simple field, Eq. (10) represents the saltation discharge (Stout, 1990).

The solution for the simple field of length s with the boundary condition $q(x = 0) = 0$ is:

$$q = q_c[1 - \exp(-c_{en}s)] \tag{11}$$

Many variations have been proposed for saltation transport capacity equations (Greeley and Iverson, 1985). For this study, one of the most-used was selected and has the form:

$$q_c = C_s u_*^2 (u_* - u_{*t}) \tag{12}$$

where C_s = saltation discharge coefficient (MT^2/L^4), u_{*t} = soil surface dynamic threshold friction velocity, i.e., threshold with saltation impacts, (L/T).

By modifying two parameters, Eq. (11) also can be used to predict the saltation discharge on the simple field with flat residue cover.

First, residue cover raises the threshold velocity. To obtain values, wind tunnel measurements were made of static threshold friction velocities, u_{*ts}, (i.e., threshold without saltation impacts) at 6, 14, 31, and 60 percent cover of flat random wheat stalks, and then the dynamic threshold friction velocity was computed as (Bagnold, 1941):

$$u_{*t} = 0.8u_{*ts} \tag{13}$$

The data were fitted to a prediction equation to give (Fig. 2):

$$u_{*t} = (0.5 + 0.96F_c - 1.046F_c^2 + 0.433F_c^3)^2 \tag{14}$$

where F_c = fraction of soil covered by flat residue cover.

The u_{*t} of the bare, 0.29–0.42 mm-diameter, quartz sand was 0.26 m/s, and the u_{*t} increased nonlinearly with residue cover.

Second, the emission coefficient is decreased by the residue cover and a modified value can be calculated as:

$$C_{env} = C_r(C_{en}) \tag{15}$$

where C_{env} = coefficient of emission for surface with flat residue cover (1/L), and C_r = ratio of emission coefficients of covered to bare surfaces.

Using data and equations reported by Lyles and Allison (1981) for soil loss from wind tunnel trays, soil loss as a function of cover was cal-

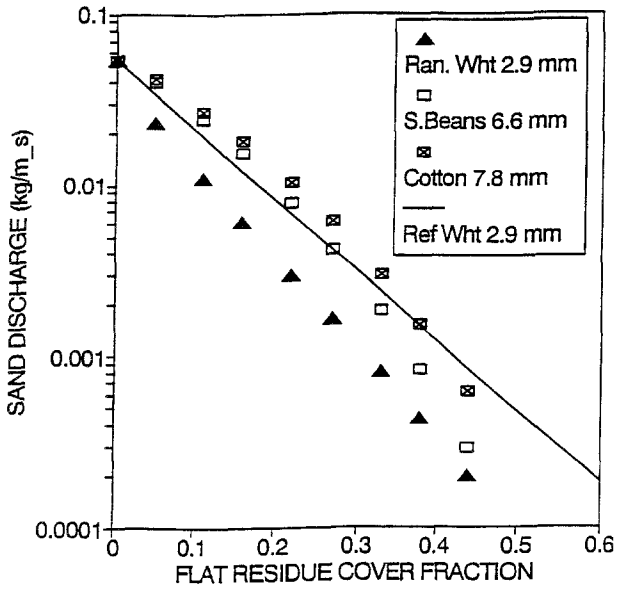

Fig. 3. Calculated sand discharge from a wind tunnel tray as a function of flat residue covers of various diameters (data from Lyles and Allison, 1981)

culated (Fig. 3). At a constant fraction of cover, the results showed that soil loss increased somewhat as residue diameters increased. For this study, the tray soil loss of the reference wheat was used to obtain values for q. Equation (11) then was used to compute C_r at selected cover levels (Fig. 2). The u_{*t} were used with the two lowest cover levels, whereas u_{*ts} were used at the highest cover levels in calculating C_r. The u_{*ts} was used at the highest cover levels, because the soil surface was largely sheltered by the residue from saltation impacts. The sand grains have an average impact angle of about 12 degrees above horizontal (Hagen, 1991b). A prediction equation also was fitted to the calculated data to give:

$$C_r = 0.075 + 0.934 \exp\left(\frac{-F_c}{0.149}\right) \tag{16}$$

The preceding equations permit direct calculation of the saltation discharge from a simple field with various levels of flat residue cover.

For a simple field with sandy soil and standing residue, a similar analysis to that for flat cover was reported in detail by Hagen and Armbrust (1994). Only a brief outline will be presented here. In this case, the friction velocity and the threshold friction velocities used in the saltation discharge equations are those at the soil surface below the standing residue. With this restriction, the saltation discharge can be modeled as:

$$\frac{dq}{dx} = c_{ens}(q_c - q) - Tq \tag{17}$$

where q_c = saltation discharge transport capacity without stalk interception (M/LT), c_{ens} = emission coefficient with standing residue ($1/L$), and T = interception coefficient of standing residue ($1/L$).

The interception coefficient for standing residue with the bulk of the saltation below the residue height is:

$$T = C_t \frac{\mathrm{SAI}}{h} \tag{18}$$

where C_t = interception coefficient of individual stalks, value about 1.

The basal area occupied by the standing residue is generally small, so c_{ens} differs little from that of the bare surface. For standing residue, we estimated that emission is restricted for two residue diameters downwind, and c_{ens} can be estimated as:

$$c_{ens} = c_{en}\left(\frac{1 - 0.0023\, D\, \mathrm{SAI}}{\mathrm{h}}\right) \tag{19}$$

Finally integration of equation 17 over the field length, 1, with initial condition $q(x = 0) = 0$ gives:

$$q = q_c \frac{c_{env}}{c_{env} + T}\{1 - \exp[-(c_{ens} + T)1]\} \qquad \Phi\Omega$$

Because the stalks do not affect q_c, it can be estimated from the same transport capacity equation used for the flat residue surface. To determine the friction velocity at the soil, u_{*0}, and calculate transport capacity, an empirical equation was fitted to data to give (Hagen and Armbrust, 1994):

$$\frac{u_{*0}}{u_*} = 0.86 \exp\left[\frac{-\mathrm{SAI}}{0.0298}\right] + 0.25 \exp\left[\frac{-\mathrm{SAI}}{0.356}\right] \tag{21}$$

Raupach (1992) reviewed the problem of drag partitioning among surface elements and developed theoretical prediction equations. Those equations based on hemisphere data of Gillette and Stockton (1989) and cylinder data of Marshall (1971), along with predictions of Eq. (21), are

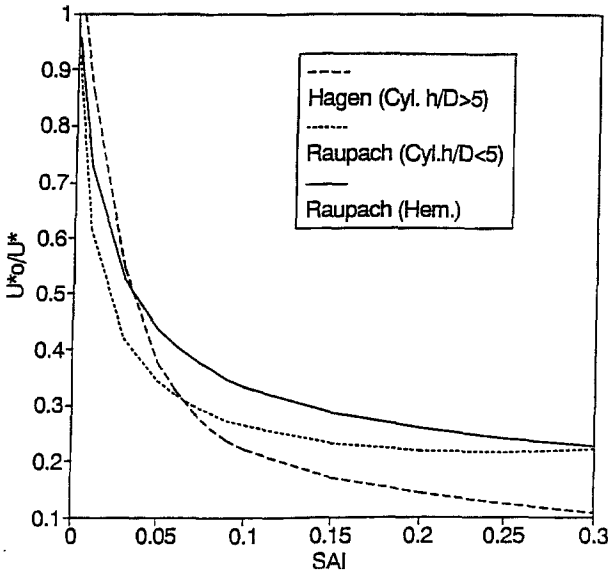

Fig. 4. Predicted ratios of mean friction velocity on intervening soil surface to that above the roughness elements for standing cylinders and hemispheres as a function of their silhouette area

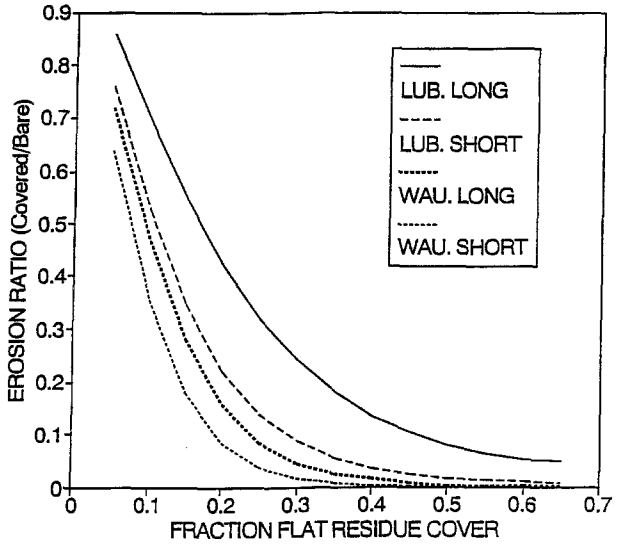

Fig. 5. Calculated ratio of erosion from covered and bare sandy fields as a function of flat residue cover on long and short fields at Lubbock, TX and Wausau, WI

shown in Fig. 4. The results indicate that tall, thin cylinders (standing residue, $h/D > 5$) provided less soil protection than short cylinders ($h/D < 5$) at low SAI, but more protection at high SAI.

Finally, the wind climate interacts with the flat and standing residues to determine the overall level of protection. To determine average saltation discharge (Q) in a specific wind climate, one must integrate over the frequency distribution of friction velocities to give:

$$Q = \int_{u_{*ts}}^{u_{*(\max)}} q(u_*, 1) f(u_*) du_* \tag{22}$$

where $f(u_*)$ = the probability density function of the friction velocity at the field surface.

Because surface wetness may periodically increase u_{*t}, the value of Q from Eq. (22) overestimates erosion. However, one may assume that the fractions of time in which wetness reduces erosion are about equal on sparsely vegetated and bare sandy surfaces. Hence, the effect of residue on wind erosion can be characterized by the dimensionless erosion ratio (R_v),

$$R_v = \frac{Q_v}{Q_b} \tag{23}$$

where the subscripts v and b refer to the residue-covered and bare surfaces, respectively.

To calculate R_v for standing and flat residues, a system of equations for various residue levels was entered into MATHCAD software (Mathsoft, 1993) and numerically integrated.

3. Results and Discussion

3.1 Flat Residue Cover Protection

In general, the erosion ratio, R_v, decreased nonlinearly as flat residue cover increased (Fig. 5). Flat cover reduces wind erosion by three mechanisms. First, it increases the static threshold velocity at which erosion begins compared to the bare surface. Second, as wind speed increases above the threshold, the transport capacity is restricted by an increased dynamic threshold velocity, on the covered surface compared to the bare surface. On long fields, these two mechanisms act to reduce the overall transport capacity of soil by effectively reducing the portion of wind energy available for soil movement.

The absolute difference between static and dynamic threshold friction velocities increases as flat cover increases. The probable explanation is that, once sand grains are emitted and begin saltating, they increasingly impact on residue cover as the cover increases. The saltating grains rebounding from cover likely retain more kinetic energy than grains striking the sand surface, because they are

rebounding from a solid surface in a region subject to the maximum wind stress. Conversely, the emission coefficient is reduced, because the soil surface is sheltered from both the grain impacts and wind stress.

The third erosion reduction mechanism occurs only on short fields. On short fields, i.e., short distance along the wind direction, the reduction in the emission coefficient with increasing cover also contributes to a reduction in R_v. This occurs because the cover increases the downwind distance needed to attain transport capacity. Thus, on short fields, the bare field will be closer to transport capacity than the covered field. The distance to transport capacity, s_{max}, on bare, sandy fields is typically 50 to 200 m. The short-field results in Fig. 5 are for field lengths of $0.4\, s_{max}$. When flat cover is the major erosion-control mechanism for a sandy field, there appears to be significant value in using trap strips, wind barriers, or other devices to periodically trap the saltating soil and keep the effective field length short. This allows the mechanism of reduced emission coefficient to contribute to erosion control. It also helps prevent burial of the exposed residues.

Flat cover fractions less than 0.05 are probably of little value in controlling wind erosion on highly erodible sands. Also, flat residues must remain on the field surface during erosion to be effective. Thus, leaves and other low density residue that are not anchored may not contribute significantly to the effective portion of the flat cover.

3.2 *Standing Residue Protection*

For standing residues, the erosion ratio decreased non-linearly with increasing silhouette area index, SAI, of the residue (Fig. 6). The conditions illustrated are for cylindrical residue, uniformly spaced, with a height of 200 mm and a diameter of 20 mm. Although a flat cover fraction of 0.05 provided little protection, the same residue standing to provide an SAI of 0.05 was highly effective in reducing wind erosion. The major erosion-control mechanism of standing residue is to reduce the friction velocity at the underlying soil surface below the threshold friction velocity. Thus, the surface does not erode, except during the fastest winds.

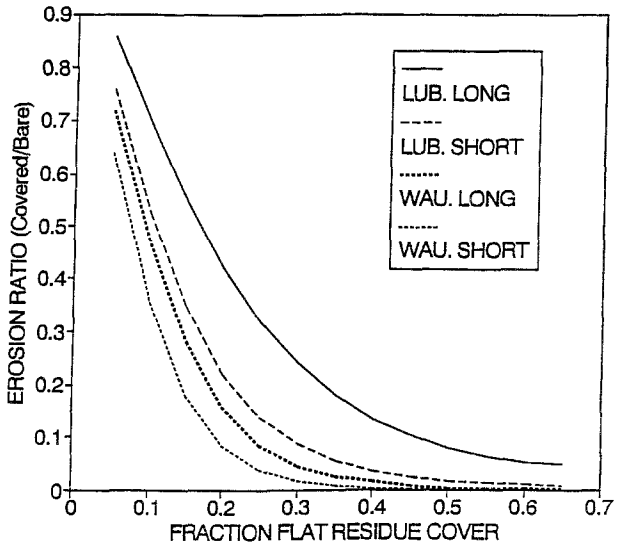

Fig. 6. Calculated ratio of erosion from covered and bare sandy fields as a function of standing residue silhouette area with saltation interception ($T > 0$, wind crossing rows) and without ($T = 0$, wind parallel rows) at Lubbock, TX and Wausau, WI

During the fastest winds, the transport capacity is reduced, compared to the bare surface, and a portion of the saltating material is intercepted by the stalks. The effect on R_v of interception by stalks is shown by the difference between the $T = 0$, (no interception) and $T > 0$ (interception) lines in Fig. 6. When wind direction is parallel to the crop rows, T approaches the minimum value.

The standing residue had little effect on the surface emission coefficient. Hence, for both the covered and bare surfaces, the downwind distance to reach transport capacity was about equal. As a result, field length did not affect R_v. Further, very low amounts of standing residue may cause a local acceleration of the friction velocity and, thus, increase R_v slightly above 1.

As noted, the results (Fig. 6) are for a uniformly spaced residue. However, residues in the field typically are not uniformly spaced, because of selected row-spacings and lodging caused by harvest and decomposition. Although studies are not available to assess the impact, a high degree of nonuniformity in spacing undoubtedly will promote interference among residue wakes and, thus, reduce erosion control by standing stubble.

Winds parallel to the row direction also may channel the flow and increase the friction velocity at the surface. Attempts to study this phenomenon in wind tunnels have largely failed, and outdoor

experiments appear necessary to quantify the effects. Hence, the R_v in Fig. 6 should be viewed as the best attainable with a given level of standing residue in the selected wind regimes.

4. Conclusions

Erosion-control mechanisms of flat residue include restricting soil emission from the surface and increasing threshold wind speeds. A minimum of 30 to 60 percent flat cover is needed to provide adequate control on highly erodible sands. The control level by flat residue can be increased by using short fields.

Erosion-control mechanisms of standing residue include reducing the soil surface friction velocity and intercepting saltating soil. Standing residue is more effective than flat residue, and 5 percent vertical silhouette area of standing residue per unit horizontal area provides adequate control in low and moderate wind regimes.

References

Apt, K. E., 1976: Applicability of the Weibull distribution to atmospheric radioactivity data. *Atmos. Environ.*, **10**, 777–782.

Bagnold, R. A., 1941: *The Physics of Blown Sand and Desert Dunes*. London: Chapman and Hall, 265 pp.

Elliot, D. L., 1979: Adjustment and analysis of data for regional wind energy assessments. Paper presented at the Workshop on Wind Climate, Ashville, North Carolina, November 12–13.

Elliot, D. L., Holladay, C. G., Barchet, W. R., Foote, H. P., Sandusky, W. F., 1987: Wind energy resource atlas of the United States. DOE/CH 10093-4. Available from National Technical Information Service, Springfield, VA.

Fryrear, D. W., 1985: Soil cover and wind erosion. *Trans. Amer. Soc. Agric. Eng.*, **28**, 781–783.

Gillette, D. A., Stockton, P. H., 1989: The effect of nonerodible particles on wind erosion at erodible surfaces. *J. Geophys. Res.*, **94**, 12, 885–12, 893.

Greeley, R., Iverson, J. D., 1985: *Wind as a Geological Process*. Cambridge, England: Cambridge University Press, 333 pp.

Gregory, J. M., 1982: Soil cover prediction with various amounts and types of crop residue. *Trans. Amer. Soc. Agric. Eng.*, **25**, 1333–1337.

Hagen, L. J., 1991a: A wind erosion prediction system to meet user needs. *J. Soil Water Conserv.*, **46**, 106–111.

Hagen, L. J., 1991b: Wind erosion mechanics: abrasion of aggregated soil. *Trans. Amer. Soc. Agric. Eng.*, **34**, 831–837.

Hagen, L. J., Armburst, D. V., 1994: Plant canopy effects on wind erosion saltation. *Trans. Amer. Agric. Eng.*, **37**, 461–465.

Lyles, L., Allison, B. E., 1981: Equivalent wind erosion protection from selected crop residues. *Trans. Amer. Soc. Agric. Eng.*, **24**, 405–408.

Lyles, L., Allison, B. E., 1976: Wind erosion: The protective role of simulated standing stubble. *Trans. Amer. Soc. Agric. Eng.*, **19**, 61–64.

Mathsoft, Inc., 1993: *Mathcad 4.0 Users Guide*. Cambridge, MA: Mathsoft, Inc., 456 pp.

Marshall, J. K., 1971: Drag measurements in roughness arrays of varying density and distribution. *Agric. Meteorol.*, **8**, 269–292.

Panofsky, H. A., Dutton, J. A., 1984: *Atmospheric Turbulence*. New York: John Wiley & Sons, 397 pp.

Raupach, M. R., 1992: Drag and drag partition on rough surfaces. *Bound.-Layer Meteor.*, **60**, 375–395.

Raupach, M. R., Gillette, D. A., Leys, J. F., 1993: The effect of roughness elements on wind erosion threshold. *J. Geophys. Res.*, **98,D2**, 3023–3029.

Shaw, R. H., Pereira, A. R., 1982: Aerodynamic roughness of a plant canopy: a numerical experiment. *Agric. Meteor.*, **26**, 51–56.

Siddoway, F. H., Chepil, W. S., Armbrust, D. V., 1965: Effect of kind, amount, and placement of residue on wind erosion control. *Trans. Amer. Soc. Agric. Eng.*, **8**, 327–331.

Skidmore, E. L., Tatarko, J., 1991: Wind in the Great Plains: Speed and direction distributions by month. In: Hanson, J. D., Schaffer, M. J., Cole, C. V. (eds.) *Sustainable Agriculture for the Great Plains*. USDA-ARS, Unnumb. Pub., pp. 195–213.

Stout, J., 1990: Wind erosion within a simple field. *Trans. Amer. Soc. Agric. Eng.*, **33**, 1597–1600.

van de Ven, T. A. M., Fryrear, D. W., Spaan, W. P., 1989: Vegetation characteristics and soil loss by wind. *J. Soil Water Conserv.*, **44**, 347–349.

Woodruff, N. P., Siddoway, F. H., 1965: A wind erosion equation. *Soil Sci. Soc. Amer. Proc.*, **29**, 602–608.

Authors' address: L. J. Hagen, USDA-ARS, Wind Erosion Research Unit, Throckmorton Hall, Kansas State University, Manhattan, KS 66506, U.S.A.